Ion irradiation induced structural and electrical transition in graphene

Yang-Bo Zhou, Zhi-Min Liao, Yi-Fan Wang, Georg S. Duesberg, Jun Xu, Qiang Fu, Xiao-Song Wu, and Da-Peng Yu

---

Articles you may be interested in

Effects of Ga ion-beam irradiation on monolayer graphene
Appl. Phys. Lett. **103**, 073501 (2013); 10.1063/1.4818458

Investigation of the effect of low energy ion beam irradiation on mono-layer graphene
AIP Advances **3**, 072120 (2013); 10.1063/1.4816715

Nanostructuring graphene on SiC by focused ion beam: Effect of the ion fluence
Appl. Phys. Lett. **99**, 083116 (2011); 10.1063/1.3628341

Structural change of ion-induced carbon nanofibers by electron current flow
J. Vac. Sci. Technol. B **29**, 04E103 (2011); 10.1116/1.3591420

Correlation between structure and electrical transport in ion-irradiated graphene grown on Cu foils
Appl. Phys. Lett. **98**, 032102 (2011); 10.1063/1.3536529

Ion irradiation induced structural and electrical transition in graphene

Yang-Bo Zhou,[1] Zhi-Min Liao,[1,2,a)] Yi-Fan Wang,[1] Georg S. Duesberg,[2,3] Jun Xu,[1] Qiang Fu,[1] Xiao-Song Wu,[1] and Da-Peng Yu[1,a)]

[1]*State Key Laboratory for Mesoscopic Physics, Department of Physics, Peking University, Beijing 100871, People's Republic of China*
[2]*Centre for Research on Adaptive Nanostructures and Nanodevices (CRANN), Trinity College, Dublin 2, Ireland*
[3]*School of Chemistry, Trinity College, Dublin 2, Ireland.*

The relationship between the electrical properties and structure evolution of single layer graphene was studied by gradually introducing the gallium ion irradiation. Raman spectrums show a structural transition from nano-crystalline graphene to amorphous carbon as escalating the degree of disorder of the graphene sample, which is in correspondence with the electrical transition from a Boltzmann diffusion transport to a carrier hopping transport. The results show a controllable method to tune the properties of graphene. © *2010 American Institute of Physics*. [doi:10.1063/1.3518979]

I. INTRODUCTION

As an atom-thick two-dimensional zero-gap material, graphene exhibits novel electrical properties, such as relativistic Dirac fermions, weak antilocalization, Klein tunneling, anomalous quantum Hall effects and spin-polarized transport.[1–7] Recently, other characters including optical, mechanical and thermal properties have also been investigated.[8–11] Many applications based on graphene nanodevice have been demonstrated, such as field effect transistors, chemical and biologic sensors, quantum dot devices, super-capacitors, etc.[1, 12–16] Due to the nature of single atomic layer, the properties of graphene are susceptible to the defects, and therefore, the disordered graphene has attracted particular interests.[17] The recent investigations through Raman spectrum reveal a three-stage transition from graphite to amorphous carbon as increasing the amount of disorder in graphene.[18–20] Studies also show that different kinds of disorder suggest different carrier scattering mechanisms,[21,22] thus result in different electrical behaviors. To understand the influence of disorder on the physical properties of graphene, various methods have been introduced to produce disorder in graphene.[21–25] Via controlling the artificial disorders in graphene, the electrical properties of disordered graphene can be well understood.[23–27] However, most of current studies focused on the properties of disordered graphene with fixed amount of disorders. The dynamic evolutions of structures and properties with regulating the degree of disorder in graphene are not well understood. In this work, Ga ion irradiation was used to induce disorder in graphene and the corresponding evolution of the properties of a monolayer graphene was systematically studied via Raman spectrum, atomic force microscope (AFM), field-effect characterization and variable temperature measurements.

II. EXPERIMENT

The monolayer graphene sample was prepared by mechanical exfoliation from Kish graphite and transferred onto a p-doped Si substrate with 300 nm thick SiO_2.[3] Optical microscope and Raman spectroscopy were used to identify the monolayer graphene.[28] The patterns on graphene were defined via electron beam lithography and the electrodes of 60 nm Au were deposited. After a lift-off process, the designed graphene device was obtained and is shown in Fig. 1 by the scanning electron microscope (SEM) image.

The disorders in graphene were induced by 30 keV Ga^+ ion irradiation using a focused ion beam system (DB 235, FEI). The ion beam current was kept as a constant of 10 pA. The beam size of 10 pA current was about 40 nm. The scanning magnification was 1500x, and the corresponding exposure area was about 3.54×10^{-4} cm^2. Therefore, the exposure current density is about 28 nA/cm^2. The amount of disorder could be controlled by varying the exposure time, which is assumed to be proportional to irradiation dosage. After each experimental batch of irradiation on graphene device, Raman spectroscopy and electrical measurements were performed to characterize the disordered graphene. The Raman spectrums were collected at the same spot of the sample for different measurement batches using a 514 nm Ar^+ laser with ∼5 mW power (Renishaw micro-Raman system). We confirmed that no additional defects were produced during the laser excitation through continuously repeating the Raman measurements. The electrical measurements were carried out with the gate voltage applied to the back of Si substrate using a semiconductor characterization system (Keithley SCS 4200). AFM measurements were also accomplished using the contact mode by a scanning probe microscope system (SPI 3800N). The contact mode scanning can obtain more accurate information of the surface roughness than the tapping mode (non-contact mode), however, it also has a risk of damaging the graphene. If there is an accidental damage of graphene during AFM measurements, then it is not possible to continuously perform the Raman and transport

a)Authors to whom correspondence should be addressed. Electronic mail: liaozm@pku.edu.cn and yudp@pku.edu.cn.
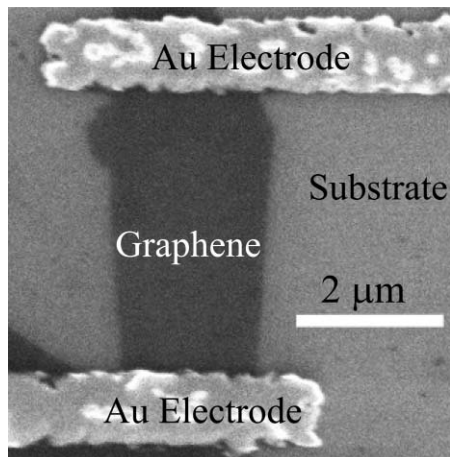
FIG. 1. SEM image of the graphene sample.

measurements. In order to avoid this unfortunate situation happening, for the AFM measurements, we chose another individual sample with exactly the same ion irradiation with the sample for Raman and transport measurements.

III. RESULTS AND DISCUSSION

The evolution of Raman spectra via ion irradiation is shown in Fig. 2. The Raman spectrum of the pristine sample indicated the existence of only a G peak at 1586 cm^{-1} and a 2D peak at the position of 2688 cm^{-1}, and the D peak associated with disorder was hardly observed. The result confirms that our sample is a monolayer graphene with little defect.[18,20,28] After the first irradiation, although only a small dosage of 1.24×10^{11} cm^{-2} was applied, the D peak appeared immediately at 1347 cm^{-1}, indicating the formation of defects in graphene. The D$'$ peak around 1624 cm^{-1} also ap-
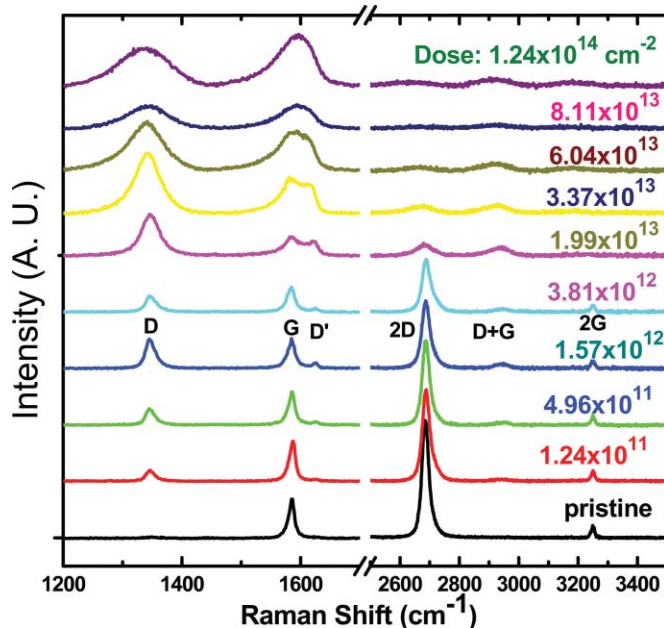

FIG. 2. The evolution of Raman spectrum of a monolayer graphene with the ion irradiation using different dosages as denoted.
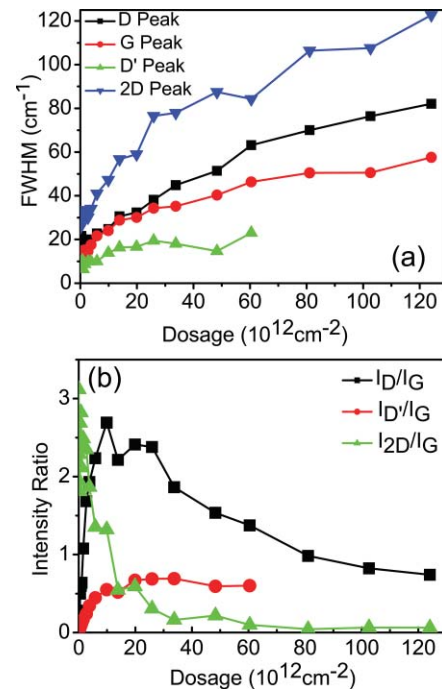

FIG. 3. (a) FWHM and (b) Raman peak intensity ratio of the D, G, D$'$ and 2D modes of graphene as a function of the irradiation ion dosage.

peared, and its intensity increased continuously with increasing the ion irradiation dose. When the dosage was larger than 8.11×10^{13} cm^{-2}, the G peak and D$'$ peak approached each other and became too close to distinguish. The evolution of full width at half maximum (FWHM) of each peak is shown in Fig. 3(a), which shows that peaks got broadening as increasing the amount of disorder.

As shown in Fig. 3(b), with increasing ion irradiation, the intensity ratio of 2D peak to G peak (I_{2D}/I_G) decreased; the intensity ratio of D$'$ peak to G peak ($I_{D'}/I_G$) increased first and then saturated; the intensity ratio of D peak to G peak (I_D/I_G) increased first and then decreased. To understand these different Raman peak intensity ratio evolutions, we consider the phonon emission and scattering process related with these peaks. 2D band and G band are due to the sp^2 symmetry. However, the G band, coming from a normal first order Raman scattering process associated with the doubly degenerate Brillouin zone center E$_{2g}$ mode,[18] which is due to the bond stretching of all pairs of sp^2 atoms in both rings and chains. On the other hand, the 2D band and D band, originating from a second-order process, are only due to the breathing modes of sp^2 atoms in rings. For the rings, as long as only one bond is broken by Ga$^+$ irradiation, the breathing mode will disappear, while the other bounds still contribute to the stretching vibration. Therefore, the 2D band decreases more rapidly than the G band and thus the I_{2D}/I_G decreases with increasing the irradiation dosage. The D$'$ peak corresponds to a defect related process, so the $I_{D'}/I_G$ ratio will increase first as increasing the amount of defect and then tends to saturation as there are sufficient defects to activate the intravalley process for the D$'$ peak.[20,28] The D peak originates from the breathing modes of the sp^2 rings and also involves a defect related scattering process, consequently, the I_D/I_G ratio will increase first as the
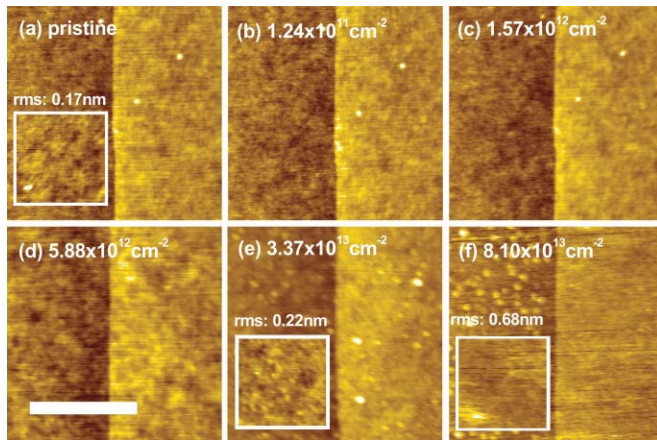
FIG. 4. The surface morphology evolution of graphene sample from low disorder to high disorder. The scale bar is 500 nm. The insets in (a), (e) and (f) display the surface roughness of graphene.
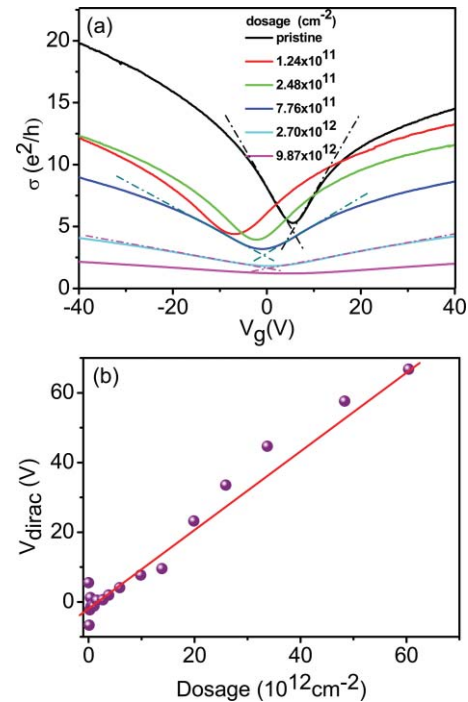

FIG. 5. (a) The characteristics of gate-voltage dependent conductivity of the graphene irradiated using different ion dosages. (b) The shifts of Dirac point versus the ion dosage.

amount of disorder increases, and then decrease because of the similar reason for the decrease of I_{2D}/I_G. More detailed behaviors of D peak evolution could be explained by the three-stage model,[18,20] that is, a transition from pure graphene to nano-crystalline graphene then to amorphous carbon. From the I_D/I_G ratio presented in Fig. 3(b), we can find that the transition inflexion from nano-crystalline graphene to amorphous disordered carbon for our sample located at an approximate dosage of 15×10^{12} cm^{-2}.

AFM measurement results further supported the structure transition. The root-mean-square-surface roughness (t_{RMS}) of the pristine monolayer graphene was around 0.17 nm, as shown in Fig. 4(a). As continuously increasing the ion irradiation dosage, no significant change of surface roughness was observed and the t_{RMS} still was about 0.17 nm, as seen from Figs. 4(b) to 4(d). However, when the dosage was much larger than the critical dosage, the t_{RMS} increased up to 0.68 nm, as shown in Figs. 4(e) and 4(f).

The structure transformation of graphene induced by ion irradiation has a significant influence on the electrical properties. Fig. 5(a) shows the gate voltage (V_g) dependence of the conductivity of the sample measured with fixed source drain voltage 50 mV. The pristine sample showed typical gate voltage dependence behavior with the Dirac point (V_{Dirac}) at 5.5 V. The positive shift of Dirac point might be caused by natural hole doping.[1–3] After the first irradiation, the Dirac point changed to –7 V, indicating an electron doping process. The gentle ion irradiation may change the SiO$_2$ surface from an oxygen-polar surface to a Si-polar surface, and thus the sample changes from p-doping to n-doping.[29,30] However, when further enhancing the ion irradiation, the Dirac point was continuously shifted toward positive gate voltage, as shown in Fig. 5(b). Since gradually adding of Ga$^+$ will destroy the graphene lattice, the defects should also have an influence on the position of Dirac point in graphene. Defects always decrease the mobility of the sample as shown in Fig. 6(a). On the other hand, defects also cause a shift of the Fermi levels by accepting or donating charge, which should have an influence on the position of Dirac point. In our sample, the defects should contribute a p-type doping, which results in the the po-

sition of Dirac point shifts continuously toward positive gate voltage in Fig. 5(a). Because the Ga$^+$ is positively charged, the charge transfer from the Ga$^+$ to the graphene can also lead to the hole doping in graphene. From Fig. 5(b), the position of Dirac point is almost proportional to the ion dosage, which may provide another evidence for the origination of p-doped graphene induced by Ga$^+$ irradiation.

The transformation of the electrical properties of graphene via ion irradiation was further analyzed by considering the carrier scattering mechanisms. To understand the scattering mechanism of our disordered graphene samples, the electron and hole carrier mobility were calculated via the tangent [the dotted lines in Fig. 5(a)] of the transfer curves.[1,21,22] As shown in Fig. 6(a), the carrier mobility decreased dramatically with increasing the ion dosage. The mobility ratio of electron to hole (μ_e/μ_h) was also calculated and showed in the inset in Fig. 6(a). The ratio was around 1.1 when the dosage was smaller than 5×10^{12} cm^{-2}, while the ratio dropped below 0.8 immediately as further enhancing the irradiation. Usually, the scattering mechanism of disordered graphene may be either charged impurity scattering or defect scattering based on Boltzmann diffusive transport.[31] For our sample, in the small irradiation dosage regime, the governing scattering should be the defect scattering, because the charged impurity scattering can produce quick drop of the μ_e/μ_h ratio which is not fact observed in our experiments.[21,32] The other evidence against the charged impurity scattering was the evolution of minimal conductivity. As shown in Fig. 6(b), the minimal conductivity decreased rapidly with increasing the ion irradiation, however, the charged impurity scattering usually results in a constant minimal conductivity.[21,31] The
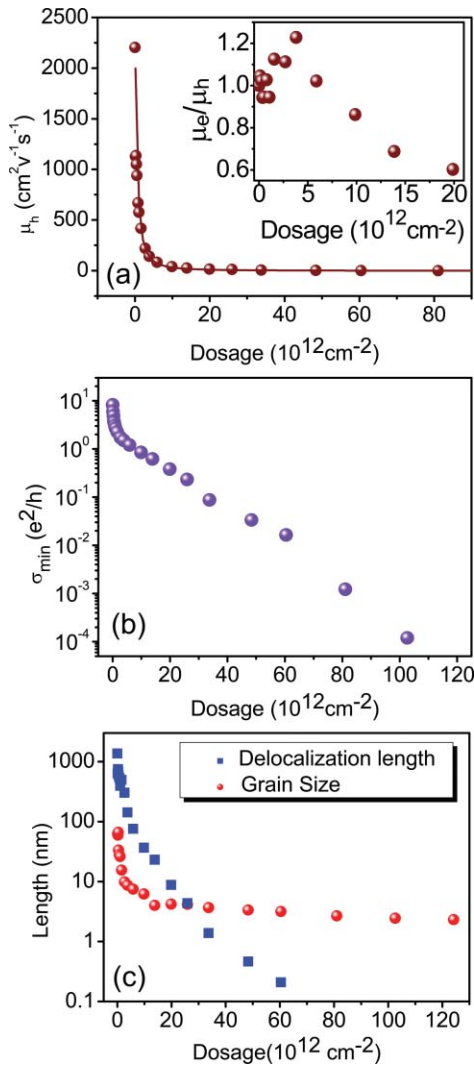
FIG. 6. (a) Hole mobility versus ion dosage. Inset: the ratio of electron to hole mobility versus dosage. (b) Minimum conductance as a function of ion irradiation dosage. (c) The delocalization length and grain size plotted vs. the ion dosage.
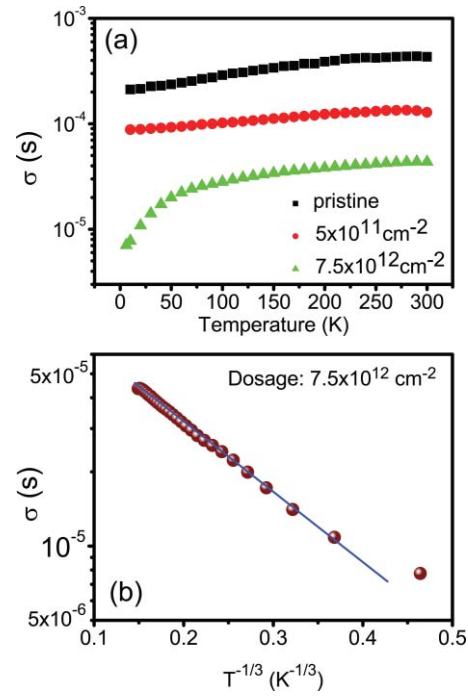

FIG. 7. (a) Temperature dependence of the conductivity of the graphene irradiated using different ion dosages. (b) The relationship between log(σ) and $T^{-1/3}$ for the highly disordered graphene.

defect scattering mechanism based on Boltzmann transport gives the formula below.[31]

$$\mu = \frac{2e}{\pi h n_d} \ln^2(k_F R), \qquad (1)$$

where h is the Planck constant, n_d is defect concentration, k_F is Femi vector, and R can be considered as the defect radius.[22,31] The simulation result according to Eq. (1) was also shown in Fig. 6(a) as the solid line, which fits well with the experiment data. The fitting results give a value of $R \sim 0.23$ nm, which is quite similar with the lattice constant of graphene and coincides with the result reported before.[22]

It should be noted that the conductivity of graphene reduced by five orders of magnitude as the irradiation dosage up to 10^{14}/cm^2. Such a low conductivity is due to strong carrier localization in the highly disordered system and the carrier transport is governed by the hopping mechanism.[33,34] The localization behavior can be described using a parameter called delocalization length ξ:

$$\xi = l \exp(\pi k_F l/2), \qquad (2)$$

where l is the mean free length which can be calculated from the conductance and the mobility data. If ξ is larger than the disordered grain size L_a, then the system is in a weak localization state. If $\xi < L_a$, then a strong localization state appears. The grain size L_a can be calculated from the Raman intensity of D peak to G peak ratio (I_D/I_G). In the low ion dosage region (below 15×10^{12} cm^{-2}), the grain size is described as[18,20]

$$L_a = [2.4 \times 10^{-10} \text{ nm}^{-3}]\lambda^4 \left(\frac{I_D}{I_G}\right)^{-1}, \qquad (3)$$

where λ is the wavelength of the excitation laser. In the high ion dosage region, L_a can be describes as[19,20]

$$L_a = \left[C(\lambda)\frac{I_D}{I_G}\right]^{-1/2}, \qquad (4)$$

where $C(\lambda)$ is a parameter related with the wavelength and the value $C(\lambda)$ is obtained using the L_a data at the transition point around 15×10^{12} cm^{-2} ion dosage. The calculated values of ξ and L_a are presented in Fig. 6(c). It clearly indicates that at the dosage smaller than 15×10^{12} cm^{-2}, $\xi > L_a$. When the dosage is larger than 15×10^{12} cm^{-2}, $\xi < L_a$. This result is well consistent with the Raman spectrum which indicates a structural transition from nano-crystalline to disordered amorphous carbon.

To more clearly reveal the transition from weak to strong localization, the temperature dependence of the conductivity was investigated. As shown in Fig. 7(a), the conductivity of the pristine and low disordered samples decreased slightly with decreasing temperature. However, for the highly disordered sample, the conductivity declined rapidly at low temperatures. The temperature dependent conductivity of the

highly disordered sample can be further analyzed using the two-dimensional Mott's variable-range hopping mechanism:

$$\sigma = \sigma_0 \exp[-(T_0/T)^{1/3}]. \tag{5}$$

The experimental data plotted as $\log(\sigma)$ vs $T^{-1/3}$ were well fitted by Eq. (5) using σ_0 and T_0 as adjustable parameters, as shown by the solid linear line in Fig. 7(b).

IV. CONCLUSIONS

In conclusion, we studied the structural and electrical evolution of disordered graphene by Ga$^+$ iron irradiation. We found a structural transition from pristine graphene to nano-crystalline graphene and to amorphous carbon, in company with the electrical transition from defect scattering in the weak localization regime to the variable-range hopping conductance in the strong localization regime. The results suggest a new method to tune the properties of graphene.

[1] K. S. Novoselov, A. K. Geim, S. V. Morozov, D. Jiang, Y. Zhang, S. V. Dubonos, I. V. Grigorieva, and A. A. Firsov, Science **306**, 666 (2004).

[2] Y. Zhu, S. Murali, W. Cai, X. Li, J. W. Suk, J. R. Potts, and R. S. Ruoff, Adv. Mater. **22**, 3906 (2010).

[3] Y. Zhang, Y. W. Tan, H. L. Stormer, and P. Kim, Nature (London) **438**, 201 (2005).

[4] K. S. Novoselov, E. McCann, S. V. Morozov, V. I. Fal'ko, M. I. Katsnelson, U. Zeitler, D. Jiang, F. Schedin, and A. K. Geim, Nat. Phys. **2**, 177 (2006).

[5] F. V. Tikhonenko, D. W. Horsell, R. V. Gorbachev, and A. K. Savchenko, Phys. Rev. Lett. **100**, 056802 (2008).

[6] N. Tombros, C. Józsa, M. Popinciuc, H. T. Jonkman, and B. J. van Wees, Nature (London) **448**, 571 (2007).

[7] A. F. Young and P. Kim, Nat. Phys. **5**, 222 (2009).

[8] K. F. Mak, M. Y. Sfeir, Y. Wu, C. H. Lui, J. A. Misewich, and T. F. Heinz, Phys. Rev. Lett. **101**, 196405 (2008).

[9] F. Wang, Y. Zhang, C. Tian, C. Girit, A. Zettl, M. Crommie, and Y. R. Shen, Science **320**, 206 (2008).

[10] C. Lee, X. Wei, J. W. Kysar, and J. Hone, Science **321**, 385 (2008).

[11] Y. M. Zuev, W. Chang, and P. Kim, Phys. Rev. Lett. **102**, 096807 (2009).

[12] Z. M. Liao, B. H. Han, Y. B. Zhou, and D. P. Yu, J. Chem. Phys. **133**, 044703 (2010).

[13] Y. Ohno, K. Maehashi, Y. Yamashiro, and K. Matsumoto, Nano, Lett. **9**, 3318 (2009).

[14] N. M. Mohanty and V. Berry, Nano Lett. **8**, 4469 (2008).

[15] L. A. Ponomarenko, F. Schedin, M. I. Katsnelson, R. Yang, E. W. Hill, K. S. Novoselovand, and A. K. Geim, Science **320**, 356 (2008).

[16] M. D. Stoller, S. J. Park, Y. W. Zhu, J. H. An, and R. S. Ruoff, Nano, Lett. **8**, 3498 (2008).

[17] P. M. Ostrovsky, I. V. Gornyi, and A. D. Mirlin, Phys. Rev. B **74**, 235443 (2006).

[18] M. A. Pimenta, G. Dresselhaus, M. S. Dresselhaus, L. G. Cancado, A. Jorio, and R. Saito, Phys. Chem. Chem. Phys. **9**, 1276 (2007).

[19] A. C. Ferrari and J. Robertson, Phys. Rev. B **61**, 14095 (2000).

[20] A. C. Ferrari, Solid State Commun. **143**, 47 (2007).

[21] J. H. Chen, C. Jang, S. Adam, M. S. Fuhrer, E. D. Williams, and M. Ishigami, Nat. Phys. **4**, 377 (2008).

[22] J. H. Chen, W. G. Cullen, C. Jang, M. S. Fuhrer, and E. D. Williams, Phys. Rev. Lett. **102**, 236805 (2009).

[23] K. Kim, H. J. Park, B. C. Woo, K. J. Kim, G. T. Kim, and W. S. Yun, Nano Lett. **8**, 3092 (2008).

[24] G. Compagnini, F. Giannazzo, S. Sonde, V. Raineri, and E. Rimini, Carbon **47**, 3201 (2009).

[25] D. C. Kim, D. Y. Jeon, H. J. Chung, Y. Woo, J. K. Shin, and S. Seo, Nanotechnol. **20**, 375703 (2009).

[26] Z. M. Liao, B. H. Han, H. Z. Zhang, Y. B. Zhou, Q. Zhao, and D. P. Yu, New. J. Phys. **12**, 083016 (2010).

[27] M. Y. Han, J. C. Brant, and Ph. Kim, Phys. Rev. Lett. **104**, 056801 (2010).

[28] A. C. Ferrari, J. C. Meyer, V. Scardaci, C. Casiraghi, M. Lazzeri, F. Mauri, S. Piscanec, D. Jiang, K. S. Novoselov, S. Roth, and A. K. Geim, Phys. Rev. Lett. **97**, 187401 (2006).

[29] Y. J. Kang, J. Kang, and K. J. Chang, Phys. Rev. B **78**, 115404 (2008).

[30] Y. Shi, X. Dong, P. Chen, J. Wang, and L. J. Li, Phys. Rev. B, **79**, 115402 (2009).

[31] T. Stauber, N. M. R. Peres, and F. Guinea, Phys. Rev. B **76**, 205423 (2007).

[32] D. S. Novikov, Appl. Phys. Lett. **91**, 102102 (2007).

[33] P. A. Lee, and T. V. Ramakrishnan, Rev. Mod. Phys. **57**, 287 (1985).

[34] S. Y. Hsu and J. M. Valles, Jr., Phys. Rev. Lett. **74**, 2331 (1995).